$$\lim_{t\to\infty}\left(\bar{c}_1\Big/\sum_{i=1}^{1}(\bar{\ })_0-\sqrt{2}\,X_{1\infty}t\right)=\lim_{t\to\infty}\frac{\sum_{i=1}^{1}(\bar{\ })_1+\sqrt{2}\left(\sum_{i=1}^{1}\sum_{j=2}^{\infty}(\bar{\ })_0+\sum_{i=2}^{\infty}\sum_{j=1}^{1}(\bar{\ })_0\right)}{\sum_{i=0}^{1}(\bar{\ })_0}$$

inasmuch as $\sum_{i=2}^{\infty}(\bar{\ })_1/\sum_{i=1}^{1}(\bar{\ })_0$ and $\sum_{i=2}^{\infty}\sum_{j=2}^{\infty}(\bar{\ })_0/\sum_{i=1}^{1}(\bar{\ })_0$ vanish exponentially as $t\to\infty$ and $\sum_{i=1}^{1}\sum_{j=1}^{1}(\bar{\ })_0/\sum_{i=1}^{1}(\bar{\ })_0=X_{1\infty}t$. It follows, therefore, that

$$\Delta_{1\infty}=\sum_{i=2}^{\infty}\frac{1}{\lambda_i^2-\lambda_1^2}\langle v\psi_1,\psi_i\rangle\left(\frac{\langle c_0|_{t=0},\psi_i\rangle}{\langle c_0|_{t=0},\psi_1\rangle}+\frac{\langle w,\psi_i\rangle}{\langle w,\psi_1\rangle}\right)+\frac{1}{\sqrt{2}}\left\{\frac{\langle c_1|_{t=0},\psi_1\rangle}{\langle c_0|_{t=0},\psi_1\rangle}-\frac{\langle c_1|_{t=0},w\rangle}{\langle c_0|_{t=0},w\rangle}\right\}$$

where $v=N_{pe}u$ and where in the product class of initial conditions the bracketed term vanishes.

The analysis for $\Delta_{2\infty}$ follows along established lines but is considerably longer. Hence we report only the result; we find that

$$\begin{aligned}\Delta_{2\infty}=&-\sum_{j=2}^{\infty}\frac{1}{(\lambda_j^2-\lambda_1^2)^2}\langle v\psi_j,\psi_1\rangle^2\\&-\frac{1}{2}\left(\sum_{j=2}^{\infty}\frac{1}{\lambda_j^2-\lambda_1^2}\langle v\psi_j,\psi_1\rangle\frac{\langle c_0|_{t=0},\psi_j\rangle}{\langle c_0|_{t=0},\psi_1\rangle}\right)^2\\&-\frac{1}{2}\left(\sum_{j=2}^{\infty}\frac{1}{\lambda_j^2-\lambda_1^2}\langle v\psi_j,\psi_1\rangle\frac{\langle w,\psi_j\rangle}{\langle w,\psi_1\rangle}\right)^2\\&+\sum_{j=2}^{\infty}\sum_{\substack{k=2\\k\neq j}}^{\infty}\frac{\langle v\psi_k,\psi_j\rangle\langle v\psi_j,\psi_1\rangle}{(\lambda_k^2-\lambda_1^2)(\lambda_j^2-\lambda_1^2)}\left(\frac{\langle c_0|_{t=0},\psi_k\rangle}{\langle c_0|_{t=0},\psi_1\rangle}+\frac{\langle w,\psi_k\rangle}{\langle w,\psi_1\rangle}\right)\\&+\sum_{j=2}^{\infty}\frac{\langle v\psi_j,\psi_1\rangle}{(\lambda_j^2-\lambda_1^2)^2}\left(\langle v\psi_j,\psi_j\rangle-\langle v\psi_1,\psi_1\rangle\right)\times\left(\frac{\langle c_0|_{t=0},\psi_j\rangle}{\langle c_0|_{t=0},\psi_1\rangle}+\frac{\langle w,\psi_j\rangle}{\langle w,\psi_1\rangle}\right)\\&+\left\{\frac{1}{2\sqrt{2}}\left(\left(\frac{\langle c_2|_{t=0},\psi_1\rangle}{\langle c_0|_{t=0},\psi_1\rangle}-\frac{1}{\sqrt{2}}\left(\frac{\langle c_1|_{t=0},\psi_1\rangle}{\langle c_0|_{t=0},\psi_1\rangle}\right)^2\right)-\left(\frac{\langle c_2|_{t=0},w\rangle}{\langle c_0|_{t=0},w\rangle}-\frac{1}{\sqrt{2}}\left(\frac{\langle c_1|_{t=0},w\rangle}{\langle c_0|_{t=0},w\rangle}\right)^2\right)\right)\right.\\&\left.+\frac{1}{\sqrt{2}}\sum_{j=2}^{\infty}\frac{1}{\lambda_j^2-\lambda_1^2}\langle v\psi_j,\psi_1\rangle\times\left(\frac{\langle c_1|_{t=0},\psi_j\rangle}{\langle c_0|_{t=0},\psi_1\rangle}-\frac{\langle c_0|_{t=0},\psi_j\rangle}{\langle c_0|_{t=0},\psi_1\rangle}\frac{\langle c_1|_{t=0},\psi_1\rangle}{\langle c_0|_{t=0},\psi_1\rangle}\right)\right\}\end{aligned}$$

where $v=N_{pe}u$ and where in the product class of initial conditions the bracketed term vanishes.

LITERATURE CITED

Courant, R., and D. Hilbert, *Methods of Mathematical Physics, I.* Interscience, New York (1966).

De Gance, A. E., and L. E. Johns, "The Theory of Dispersion of Chemically Active Solutes in a Rectilinear Flow Field," *Appl. Sci. Res.*, **34**, 189 (1978*a*).

De Gance, A. E., and L. E. Johns, "On the Dispersion Coefficients for Poiseuille Flow in a Circular Cylinder," *ibid.*, 227 (1978*b*).

Gill, W. N., and R. Sankarasubramanian, "Dispersion of a Non-uniform Slug in Time Dependent Flow," *Proc. Royal Soc. Lond.*, **A 322**, 101 (1971).

Sankarasubramanian, R., and W. N. Gill, "Unsteady Convective Diffusion with Interphase Mass Transfer," *ibid.*, **A 333**, 115 (1973).

Manuscript received December 4, 1978; revision received April 9, and accepted April 16, 1979.

Stochastic Simulation of the Motion, Breakup and Stranding of Oil Ganglia in Water-Wet Granular Porous Media During Immiscible Displacement

K. M. NG

and

A. C. PAYATAKES

Chemical Engineering Department
University of Houston
Houston, Texas 77004

The problem of immiscible displacement of oil ganglia arises in connection with oil bank formation and attrition during enhanced oil recovery with flooding. A stochastic simulation method is developed here, which enables prediction of the fate of solitary ganglia during immiscible displacement in water-wet unconsolidated granular porous media. This method takes into account the local topology of the porous medium; the initial size, shape and orientation of the oil ganglion and the capillary number. For each ganglion size, hundreds of realizations are performed with random ganglion shapes for a 100 × 200 sandpack. These results are averaged to obtain probabilities of mobilization, breakup and stranding as functions of capillary number and ganglion size. Axial and lateral dispersion coefficients are obtained as functions of the average ganglion velocity. The results from the solitary ganglion analysis can be used with the ganglion population balance equations developed in a companion publication (Payatakes, Ng and Flumerfelt, 1980) to study the dynamics of oil bank formation.

SCOPE

At the end of secondary oil recovery processes, 40 to 70% of the original amount of oil remains in the reservoir. Usually, this residual oil is dispersed throughout the porous rock in the form of small oil ganglia (nodular blobs) each of which occupies one to, say, fifteen adjoining chambers of the porous medium. The rest of the porous space is taken by brine (formation

0001-1541-80-3682-0419-$01.25.

water). Enhanced oil recovery methods are designed to mobilize this residual oil by miscible or immiscible displacement. Optimally designed micellar flooding begins as a miscible displacement process but inevitably deteriorates to a less efficient immiscible mode (Healy and Reed, 1974; Healy, Reed and Stenmark, 1976; Nelson and Pope, 1977). In a companion publication (Payatakes, Ng and Flumerfelt, 1979), the dynamic behavior of a large population of oil ganglia undergoing immiscible displacement in a water-wet granular unconsolidated porous medium was modeled with two coupled population balance equations of the birth-death type. The first of these equations applies to mobilized oil ganglia and the second to stranded ones. The entire model is based on a new porous medium model composed of a network of unit cells of the constricted tube type. Central among the parameters of the ganglion population balances are the probabilities of mobilization, breakup and stranding of oil ganglia as well as the axial and lateral dispersion coefficients. How these parameters can be calculated from stochastic realizations of the fate of solitary oil ganglia is the object of the present work.

CONCLUSIONS AND SIGNIFICANCE

A mobilization-breakup criterion is formulated that takes into account the size, shape and orientation of the ganglion, the local topology of the pore space (especially the throat size distribution) and the capillary number. Samples of representative realizations are given to illustrate the simulation method. For given ganglion size and random initial shape, hundreds of one-step (one rheon) realizations can be performed, and the outcomes can be averaged to obtain the probability of mobilization M, the probability of breakup per rheon B, and the probability of stranding per rheon S. This calculation was performed for a 100×200 sandpack, contact angle $\theta = 0$ and oil ganglion sizes ranging from one to over fifty elemental void spaces (see Payatakes, Ng and Flumerfelt, 1980). The resulting probabilities M, B and S are plotted as functions of capillary number, with the ganglion size as parameter. The breakup-mode probability density function $W(u, v)$ is also derived and plotted. Analytical expressions giving the ganglion stranding coefficient λ and the breakup coefficient ϕ as functions of the probabilities M, B and S are derived, and plots of λ and ϕ as functions of ganglion size and capillary number are given. Finally, expressions for the axial and lateral ganglion dispersion coefficients, D_z and D_x, respectively, are derived.

The present work, together with its companion publication (Payatakes, Ng and Flumerfelt, 1980) gives an approximate but detailed analysis of the dynamics of oil bank formation.

The model provides a much profounder understanding of immiscible microdisplacement than that afforded by previous work, reveals several important factors that had not been clearly discerned in the past and points the way for further research.

QUASISTATIC CRITERION FOR THE MOBILIZATION AND BREAKUP OF OIL GANGLIA

Consider a typical oil ganglion in a water-wet granular porous medium, Figure 1. Figure 1 is already a two-dimensional idealization, but this does not affect the development of the criterion. Let us assign indices 1, 2, 3, . . . to the various interfaces residing at or near throats, starting with the interface which is located furthest downstream in the direction of the negative macroscopic pressure gradient $(-\nabla P)$. Let P_{oi} and P_{wi} be the static pressure values in the oil and water phase, respectively, immediately adjacent to the i^{th} interface, and let J_i be the curvature of that interface. If one considers a single interface at a single throat separating pools of two immiscible liquids, the only stable configurations are those for which the magnitude of the curvature J is intermediate to two limiting curvatures, the drainage curvature J_{dr} and the imbibition curvature J_{imb} (Melrose, 1965). If we assume that ∇P is too small to effect mobilization of the oil ganglion, the static equilibrium at each interface is expressed by

$$P_{oi} - P_{wi} = J_i \gamma_{ow} > 0 \tag{1}$$

Neglecting hydrostatic pressure differences within the ganglion, we set

$$P_{oi} = P_{o1};\ \text{all } i \tag{2}$$

In calculations of this type, it is frequently assumed, for lack of better information, that the pressure difference between any two points in the aqueous phase can be calculated simply as the inner product of the macroscopic pressure gradient and the position vector difference. In our notation

$$P_{wi} - P_{w1} \cong -\nabla P \cdot \vec{\Delta} L_{i1} = G \Delta L_{i1} \cos\theta_{i1} \tag{3}$$

where $\vec{\Delta} L_{i1}$ is the difference between the position vector of the i^{th} interface and the position vector of the first interface, ΔL_{i1} is the distance between the two interfaces and θ_{i1} is the angle between the vectors $\vec{\Delta} L_{i1}$ and $(-\nabla P)$. For simplicity we have set $G \equiv -\nabla P$.

Equations (1) through (3) give

$$J_i(G;\theta) = J_1(G;\theta) - \frac{G}{\gamma_{ow}} \Delta L_{i1} \cos\theta_{i1};\ \text{all } i \tag{4}$$

Suppose we increase the magnitude of the pressure gradient G very slowly, but not far enough to cause a rheon. Equations (4) are still valid at each G value (quasistatic equilibrium). The first term on the right-hand side, namely, the curvature at the downstream most interface, is positive and increases

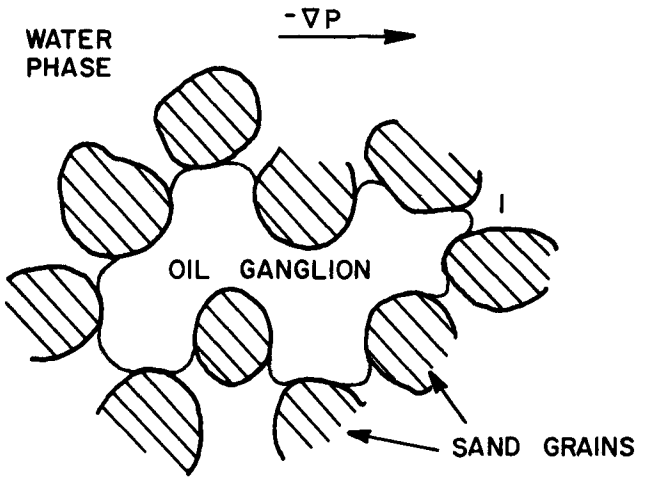

Figure 1. Two-dimensional idealization of a typical oil ganglion under conditions of incipient rheon. For the purposes of analysis, indices assigned to the various oil-water interfaces starting with the one furthest downstream.

monotonically with G, whereas the second term (including the minus sign) is negative and also increases in magnitude with G. Hence, we can separate the throats into three classes: downstream throats (small ΔL_{i1}), where an increase of G always results in a small advancement of the interface and increase of its curvature, upstream throats (large ΔL_{i1}), where exactly the opposite occurs, and midstream throats, where the curvatures remain nearly constant. For given G and θ and ganglion configuration, the system of Equations (4) contains one equation less than the number of unknowns $\{J_i; i = 1, 2, 3, \ldots\}$. This creates a closure problem. In principle, this closure problem can be solved rigorously by specifying the exact geometry of the porous medium in the neighborhood of the ganglion and by giving the ganglion volume, because then one can determine only one solution that satisfies Equations (4) as well as the fixed volume requirement. If this solution has no downstream appendix curvature that exceeds the drainage curvature of the corresponding throat, the solution can be considered as stable (we assume that one or more upstream curvatures may take values smaller than the corresponding imbibition curvature values, so long as the downstream curvatures do not exceed their drainage values). Hence, the critical value of G necessary to induce mobilization, G_{cr}, can be determined by gradually increasing the value of G and checking the stability of all downstream interfaces until one becomes unstable. Clearly, this approach would require quite laborious calculations and would be ill suited for repeated use in stochastic simulations.

A less rigorous but much more convenient approach is developed below (the concepts are akin to those in Melrose and Brandner, 1974). Let K be the as yet unknown index of the throat through which the hygron will take place. We will assume that under incipient mobilization conditions ($G = G_{cr}$) the K^{th} throat is the one in which the curvature is closest to the smallest value possible in the throat in which the interface resides:

$$J_K(G_{cr};\ \theta) \cong J_{lb,K}(\theta),\ J_j(G_{cr};\ \theta) > J_{lb,j}(\theta);\ j \neq K \tag{5a}$$

Here, $J_{lb,j}(\theta)$ is the lower bound of J_j, and it will be estimated as the curvature in a cylindrical tube with diameter equal to the effective diameter of the chamber into which the j^{th} interface resides. In terms of the model in Payatakes, Ng and Flumerfelt (1980), we set

$$J_{lb,j}(\theta) \cong \frac{4}{a_j}\cos\theta;\ \text{all } j \tag{5b}$$

In general, the value of $J_{lb,K}$ is quite small compared to the downstream drainage curvatures, and therefore an approximate estimate is adequate. This is especially true for values of θ larger than 20 deg and approaching 40 deg when, as Melrose (1965) has shown, the role of the imbibition curvatures becomes entirely subordinate to that of drainage curvatures. Equation (5) is the additional information required to resolve the closure problem of Equations (4) and is used in lieu of the more rigorous fixed ganglion volume requirement.

It is now possible to determine K by making a conceptual experiment (sensitivity analysis). At fixed G, let $J_1^{(j)}$ be the curvature value of the downstream most interface resulting, if we force the curvature of the j^{th} upstream interface to take its minimum value $J_{lb,j}$ and at the same time we block all other downstream throats to prevent any rheons through them from taking place. From Equation (4)

$$J_1^{(j)}(G;\theta) = J_{lb,j}(\theta) + \frac{G}{\gamma_{ow}}\Delta L_{j1}\cos\theta_{j1};\ \text{all } j \neq 1 \tag{6}$$

Let

$$J_{1,\min}(G;\theta) \equiv \max\{J_1^{(j)}(G;\theta);\ j = 2,3,\ldots\} \tag{7}$$

$J_{1,min}(G;\theta)$ is the minimum possible value of $J_1(G;\theta)$; otherwise at least one of the curvatures $\{J_j(G;\theta); j = 2, 3, \ldots\}$ would take a value less than its lower bound, $J_{lb,j}$. Hence

$$J_1(G;\theta) \geqq J_{1,\min}(G;\theta) \tag{8}$$

Obviously, in our hypothetical sensitivity analysis, when G reaches its critical value a xeron will take place through the downstream most throat. This hypothetical critical value of G can be assumed to be close to the actual critical value G_{cr}, and therefore

$$J_1^{(K)}(G_{cr};\theta) = J_{1,\min}(G_{cr};\theta) = \max\{J_1^{(j)}(G_{cr};\theta);\ j = 2,3,\ldots\} \tag{9}$$

Thus, the hygron index K is shown to be that for which $J_1^{(j)}(G_{cr};\theta)$ becomes maximum, and it can be determined readily if G_{cr} is known (which it is not at this point). It can be verified easily that according to Equation (9), J_K is the first curvature to reach its minimum possible value as $G \to G_{cr}$, in agreement with Equation (5).

In order to determine a first approximate to G_{cr}, we set

$$G_{cr} \cong G_{cr}^{(0)} = \frac{\gamma_{ow} J_{dr,1}(\theta)}{L_p} \tag{10}$$

Drainage curvatures are given by

$$J_{dr,i} \cong \frac{4}{d_i}\cos\theta\ ;\ \text{all } i \tag{11}$$

Inserting G_{cr} from Equation (10) into Equations (9), we determine K. At this point there is still some uncertainty as to whether the value of K just determined is the correct one, since we used an approximation for G_{cr} [Equation (10)]. Improvement by iteration may be possible, as will be seen below.

The index of the throat through which the oil actually invades the space of water (xeron), if G exceeds G_{cr}, is denoted by I. We have

$$J_{dr,I}(\theta) = J_I(G_{cr};\theta)\ ,\quad J_{dr,i}(\theta) > J_i(G_{cr};\theta)\ ;\ i \neq I \tag{12}$$

Now Equations (4) and (5) give

$$J_i(G_{cr};\theta) = J_1(G_{cr};\theta) - \frac{G_{cr}}{\gamma_{ow}}\Delta L_{i1}\cos\theta_{i1}\ ;\ i \neq K$$

$$J_{lb,K}(\theta) = J_1(G_{cr};\theta) - \frac{G_{cr}}{\gamma_{ow}}\Delta L_{K1}\cos\theta_{K1} \tag{13}$$

which can be solved to obtain

$$J_i(G_{cr};\theta) = J_{lb,K}(\theta) + \frac{G_{cr}}{\gamma_{ow}}\Delta L_{Ki}\cos\theta_{Ki}\ ;\ i \neq K \tag{14}$$

Equations (12) and (14) give

$$J_{dr,I}(\theta) = J_{lb,K}(\theta) + \frac{G_{cr}}{\gamma_{ow}}\Delta L_{KI}\cos\theta_{KI}$$

$$J_{dr,i}(\theta) > J_{lb,K}(\theta) + \frac{G_{cr}}{\gamma_{ow}}\Delta L_{Ki}\cos\theta_{Ki}\ ;\ i \neq I \tag{15}$$

For the ganglion under consideration, we define a set of appendix mobility factors:

$$\beta_{Ki}(\theta) \equiv \frac{\Delta L_{Ki}\cos\theta_{Ki}}{[J_{dr,i}(\theta) - J_{lb,K}(\theta)]};\ \text{all } i \tag{16}$$

If we recall Equations (5) and (11) and set

$$J_{dr,i}^{0} \equiv J_{dr,i}(0) = \frac{4}{d_i},\ J_{lb,K}^{0} \equiv J_{lb,K}(0) = \frac{4}{a_i} \tag{17}$$

Equation (16) becomes

$$\beta_{Ki}(\theta) \cong \frac{\Delta L_{Ki}\cos\theta_{Ki}}{(J_{dr,i}^{0} - J_{lb,K}^{0})\cos\theta};\ \text{all } i \tag{18}$$

Equations (15) and (18) together give

$$\beta_{Ki} < \beta_{KI} = \frac{\gamma_{ow}}{G_{cr}}\ ;\ i \neq I \tag{19}$$

Hence, the index I is shown to be the one for which

$$\beta_{KI} = \max\{\beta_{Ki};\ i = 1,2,\ldots\} \tag{20}$$

and can be determined from Equation (20), since the hygron index K is tentatively known.

A better approximation to G_{cr} is now possible by setting

$$G_{cr} = \frac{\gamma_{ow}}{\beta_{KI}} \tag{21}$$

At this point one must use the updated value of G_{cr} to determine an undated value of K from Equation (9). If the new value of K differs from the value of the first iteration, the entire procedure is repeated until both K and I values remain unchanged.

In the way of a summary, the mobilization breakup criterion is given below in algorithm form, as it applies to the porous medium model developed in Payatakes, Ng and Flumerfelt (1980).

1. Assign indices $i=1,2, \ldots, N_{guc}$ to all gate unit cells starting with the one furthest downstream.
2. Determine a first approximation to the value of the critical pressure gradient needed for mobilization, G_{cr}, from Equation (10).
3. Determine the hygron index K from Equation (9).
4. Determine the xeron index I from Equation (20).
5. Determine a better approximation to G_{cr} from Equation (21).
6. Use the updated value of G_{cr} and iterate steps 3 to 5 until no more changes in K, I and G_{cr} are observed. As it turns out, one to two iterations are usually all that is needed. Then proceed to step 7.
7. Mobilization will take place if the applied pressure gradient ∇P_{ap} exceeds G_{cr} in magnitude:

$$\begin{aligned} -\nabla P_{ap} > G_{cr} &\rightarrow \text{mobilization} \\ -\nabla P_{ap} < G_{cr} &\rightarrow \text{stranding} \end{aligned} \tag{22}$$

This criterion can also be expressed as

$$N_{am} \equiv \frac{|\nabla P_{ap}|\Delta L_{KI}\cos\theta_{KI}}{\gamma_{ow}(J^0_{dr,i}-J^0_{lb,K})\cos\theta}$$

$$= \beta_{KI}\frac{|\nabla P_{ap}|}{\gamma_{ow}} \begin{cases} >1 \rightarrow \text{mobilization} \\ <1 \rightarrow \text{stranding} \end{cases} \tag{23}$$

Equivalently

$$\left.\begin{aligned} N_{Ca} \equiv \frac{\mu_w V_f}{\gamma_{ow}} > \frac{k_{rw}k}{\beta_{KI}} &\rightarrow \text{mobilization} \\ N_{Ca} \equiv \frac{\mu_w V_f}{\gamma_{ow}} < \frac{k_{rw}k}{\beta_{KI}} &\rightarrow \text{stranding} \end{aligned}\right\} \tag{24}$$

If the hygron index K is located somewhere in the middle of the ganglion, and the ganglion thickness at that point consists of only one CEVS (the one about to be invaded by the wetting phase), the oil ganglion fissions into two daughter ganglia (very infrequently into three).

The present criterion is more realistic than and supercedes that developed in Paytakes et al. (1977) and used in Payatakes et al. (1978 *a, b*). That earlier version of the criterion was found to exaggerate somewhat the role of the upstream interface curvatures.

STOCHASTIC SIMULATION OF THE FATE OF SOLITARY GANGLIA

In order to initiate a stochastic realization of the fate of a ganglion, one needs to specify, among other things, the initial shape of the ganglion. To this end we chose to generate random initial ganglion shapes. This can be done readily by considering the porous medium model network and by randomly assigning oil to conceptual elemental void spaces (CEV's) until the required number of adjoining oil filled CEVS's is obtained. Two examples of computer generated two-dimensional random shapes of nine CEVS ganglia are shown in Figure 2.

The rationale behind this approach is that even though oil ganglia tend to acquire elongated configurations (see below), this tendency is spoiled by the frequent fissioning and coalescence that the ganglia undergo. Of course, there is no evidence that fission and coalescence completely overshadow a certain streamlining of the oil ganglia. For lack of experimental information, we will proceed on the assumption of completely randomly shaped ganglia. Future work may have to be modified to account for ganglion slenderization.

The algorithm for the computer aided simulation of ganglia fates is given below. For simplicity, it is based on the two-dimensional version of the cubic network. This is equivalent to assuming the pressure gradient to be parallel to one of the families of network planes and, further, to assuming that rheons normal to those planes are not permissible. To avoid any directional bias, the pressure gradient is taken parallel to the bisector of the right angle formed by the two main axes on the network plane.

1. Specify the constriction size distribution and other pertinent geometric characteristics of the porous medium model (see

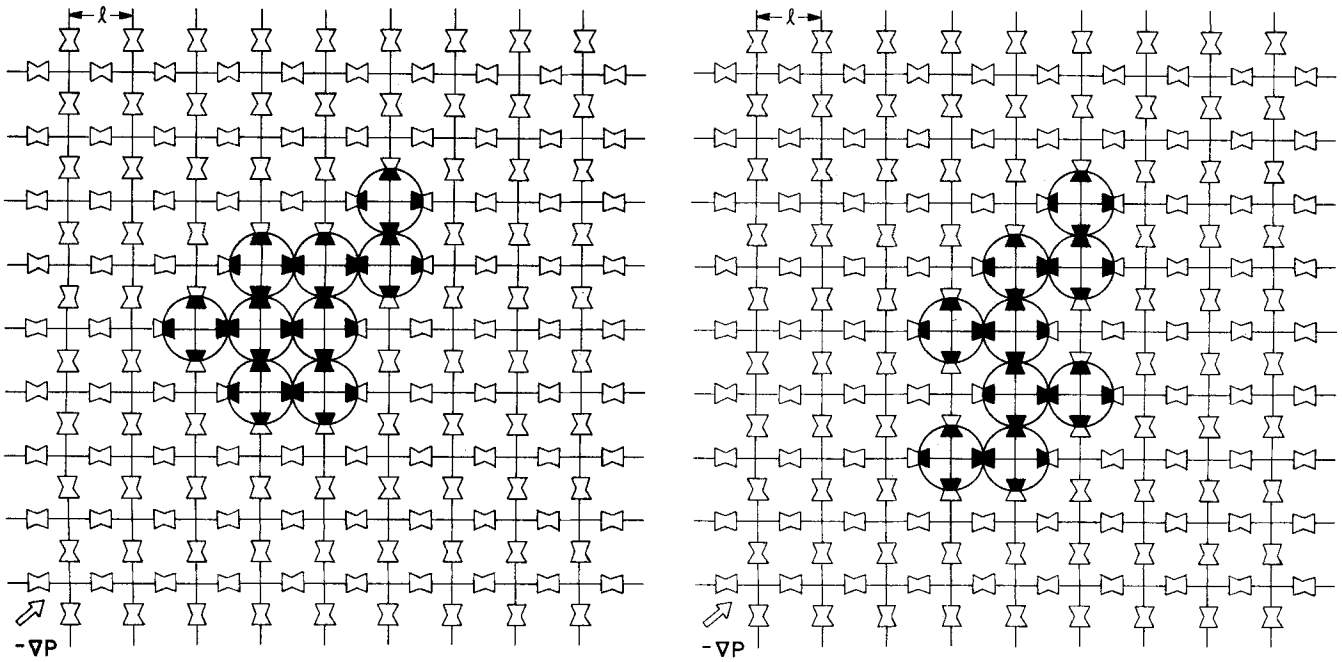

Figure 2. Two examples of computer generated two-dimensional random shapes of nine CEVS ganglia.

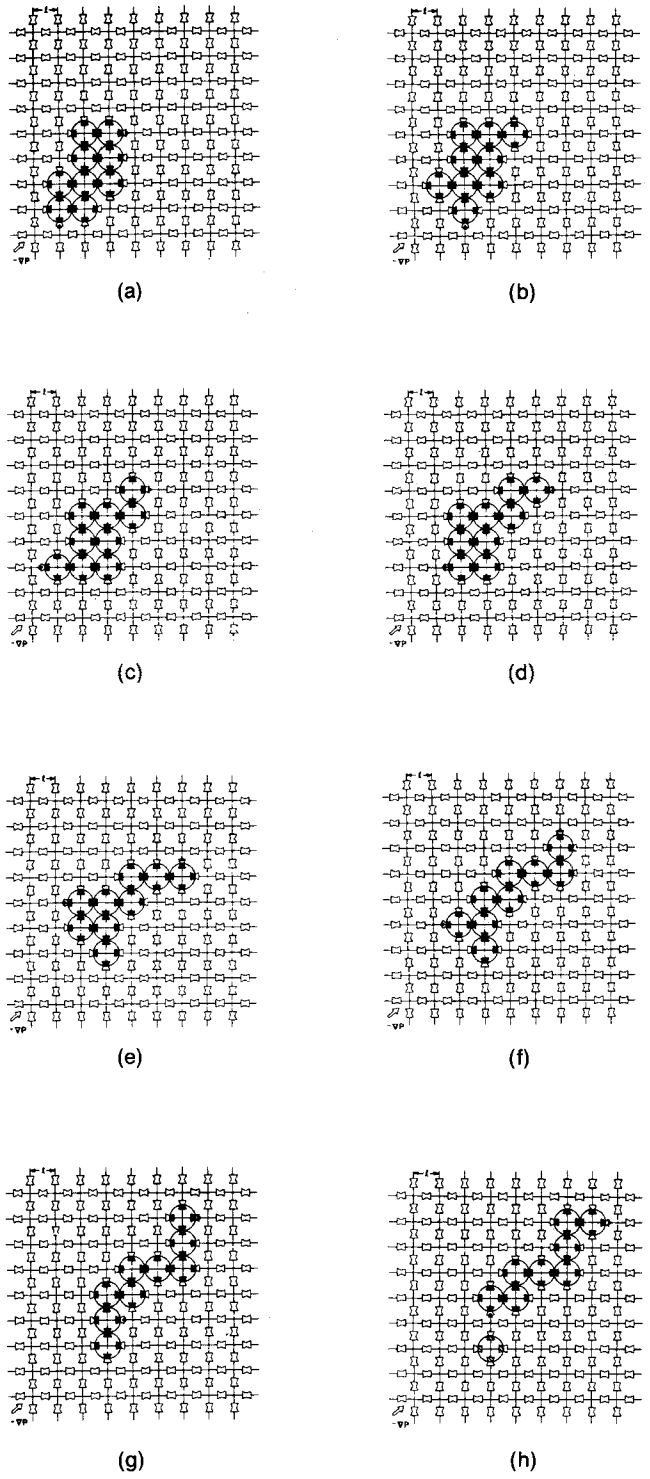

Figure 3. Typical realization of the fate of a nine CEVS ganglion introduced randomly into a 100 × 200 sandpack for capillary number N_{Ca} = 1.07 × 10^{-3}. (a) Initial ganglion; (b) through (g) show the positions and shapes of the ganglion resulting from six successive rheons. (h) With the seventh rheon the ganglion fissions in two daughter ganglia. It so happens here that the small daughter ganglion remains stranded whereas the large one takes at least one more step.

Payatakes, Ng and Flumerfelt, 1980) corresponding to the porous medium prototype under consideration.

2. Assign random values to the throats of all unit cells in a sufficiently large segment of the model network based on the constriction size distribution (see Payatakes, Ng and Flumerfelt, 1980).

3. Specify the capillary number, N_{Ca}, value.

4. Specify the desired ganglion size (say, nine CEVS).

5. Generate a randomly shaped ganglion of the specified size, within the porous medium model network.

6. Record the present position of the ganglion (coordinates of all CEVS's)

7. Apply the mobilization-breakup criterion. If no mobilization is predicted, go to step 9 and record stranding at the present position. If breakup is predicted, go to step 9 and record breakup and the mode of breakup (sizes and positions of daughter ganglia). If mobilization without breakup occurs, update the position of the ganglion (delete coordinates of the CEVS invaded by water and add the coordinates of the CEVS invaded by the oil ganglion); then go to step 8.

8. Iterate steps 6 to 8 until breakup or stranding occurs.

9. Stop the computations and report the terminal event (stranding or breakup).

It should be added that step 2 is used for convenience and that it leads to core memory waste, especially in cases of sizeable ganglia requiring large network domains. In such cases it is far better to assign dimensions only to the gate unit cells as needed; the results are equivalent.

Sample Stochastic Simulation of Ganglion Fate

As a basis for sample stochastic simulations we chose a 100 × 200 sandpack of porosity $\epsilon = 0.395$. The constriction size distribution and other pertinent geometric parameters were determined in Payatakes, Ng and Flumerfelt (1980). A typical realization of the fate of a nine CEVS ganglion in the 100 × 200 sandpack with $\theta = 0$ and with $N_{Ca} = 1.07 \times 10^{-3}$ is shown in Figure 3. The ganglion undergoes seven rheons before it fissions into two daughter ganglia. It so happens in this example that one daughter ganglion remains stranded, while the other executes at least one more rheon.

General Conclusions

In general, mobilized oil ganglia demonstrate a definite tendency to become long and slender as they undergo successive rheons and also to align themselves closely with the macroscopic flow. In addition to these observations, the main lesson to be learned is that almost certainly, and after relatively few rheons, solitary oil ganglia either get restranded without fissioning or first fission into daughter ganglia and then the latter get stranded. Hence, very small microdisplacement efficiency is expected in the absence of vigorous coalescence between colliding ganglia, even in the case of large ganglion populations (see also Payatakes, Ng and Flumerfelt, 1980). Frequent collisions and coalescence between ganglia tend to produce fewer and larger ganglia, which have higher velocities and smaller probabilities of stranding. If the effects of collison coalescence on the ganglion population dominate those of breakup restranding, the conditions for oil bank formation are favorable. Otherwise the mobilized oil ganglia deteriorate by breakup into smaller and more numerous ones, which eventually get stranded anew.

Insufficient rates of coalescence can be caused by small probability of coalescence given a collision between two ganglia, due to stabilizing films of dissolved or suspended substances at oil-water interfaces; small rate of collisions between ganglia due to a sparse initial population (small residual oil saturation); a combination of the two.

That coalescence plays a central role in determining the efficiency of micellar flooding is a fact known to reservoir engineers both from laboratory and field tests. In more recent years, Wasan and his co-workers (1978, 1979) have focused attention on this relation and its importance. The results of the present study are in accord with previous experience; beyond this, they make possible for the first time a fundamental quantitative assessment of the role of coalescence, as well as of other physicochemical, geological and operational factors on microdisplacement efficiency.

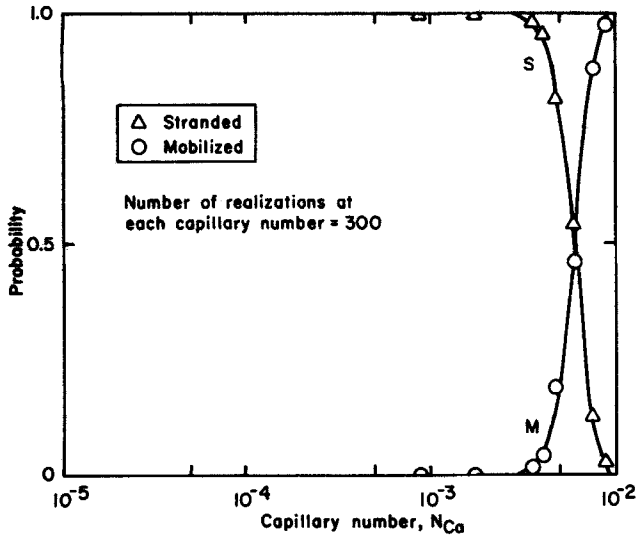

Figure 4. Plot of the probabilities of mobilization M and stranding per rheon S for one CEVS ganglia in a 100 × 200 sandpack vs. capillary number.

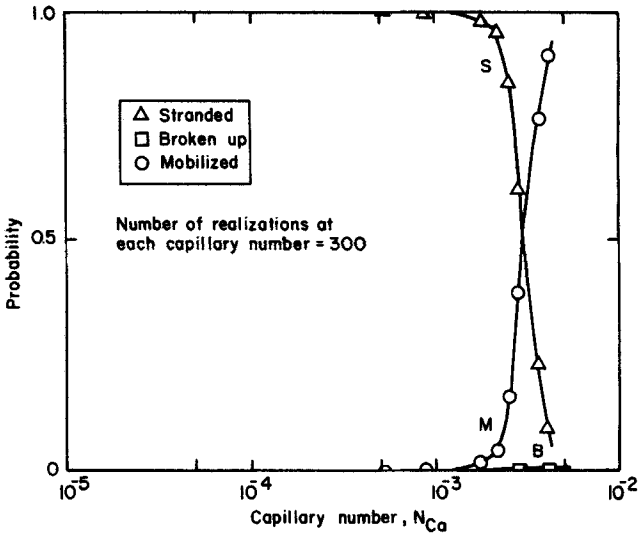

Figure 5. Plot of the probabilities of mobilization M, breakup per rheon B and stranding per rheon S for two CEVS ganglia in a 100 × 200 sandpack vs. capillary number.

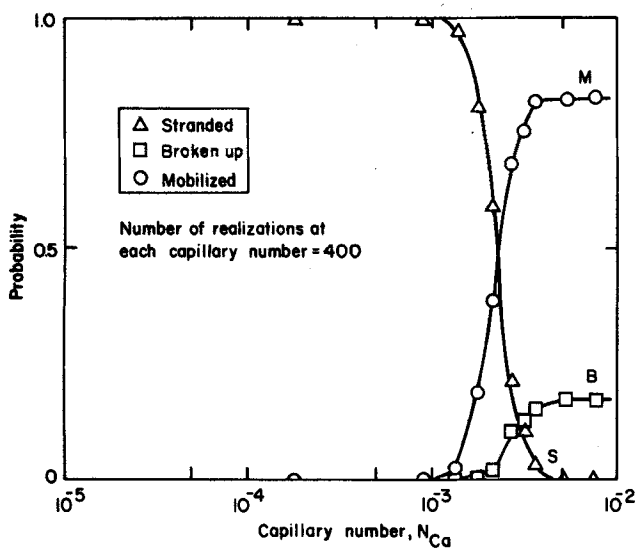

Figure 6. Plot of the probabilities of mobilization M, breakup per rheon B and stranding per rheon S for three CEVS ganglia in a 100 × 200 sandpack vs. capillary number.

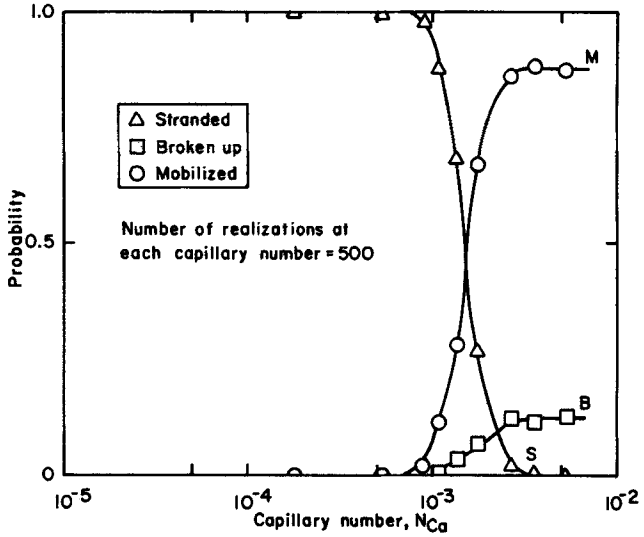

Figure 7. Plot of the probabilities of mobilization M, breakup per rheon B and stranding per rheon S for five CEVS ganglia in a 100 × 200 sandpack vs. capillary number.

PROBABILITIES OF MOBILIZATION, BREAKUP AND STRANDING

Consider a porous medium in which the aqueous phase is moving under the influence of a pressure gradient ∇P. Suppose now that we introduce into this medium a single randomly shaped oil ganglion. There are three possible events that may follow: the oil ganglion undergoes at least one rheon without breaking up in the process, the oil ganglion, or part of it, mobilizes but breakup occurs immediately and the oil ganglion remains stranded at the position in which it was placed. We will denote the probabilities of these events as M, B and S, respectively. Obviously, M, B and S are functions of all geometrical, physicochemical and operational variables that affect the fate of solitary oil ganglia. Actually, they incorporate most of the factors that govern the fate of solitary ganglia, and it is thereof that they derive their importance. Furthermore, if we accept the premise that for given ganglion size the original random ganglia shapes in the stochastic simulations are representative of the shapes that such ganglia take during their brief lives, then M, B and S can also be interpreted as

$M = Pr$ {the ganglion gets mobilized whole from its present position} (25)

$B = Pr$ {the ganglion fissions during the current rheon} (26)

$S = Pr$ {the ganglion gets stranded at its present position} (27)

irrespective of whether we consider the first rheon or a subsequent one.

Obviously

$$M + B + S = 1 \tag{28}$$

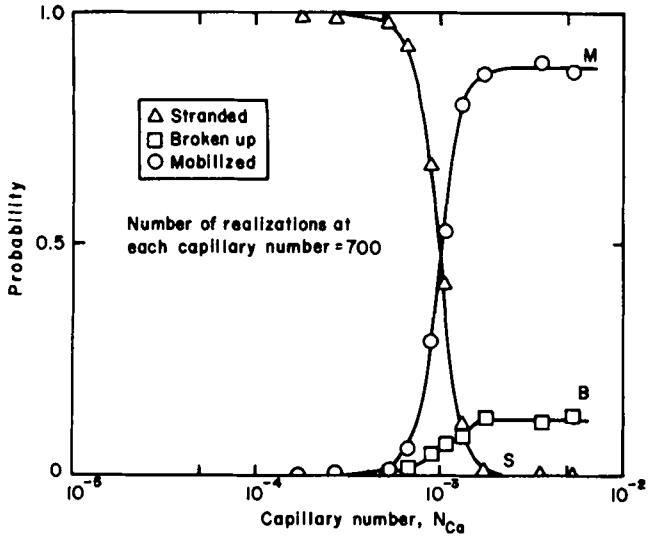

Figure 8. Plot of the probabilities of mobilization M, breakup per rheon B and stranding per rheon S for nine CEVS ganglia in a 100 × 200 sandpack vs. capillary number.

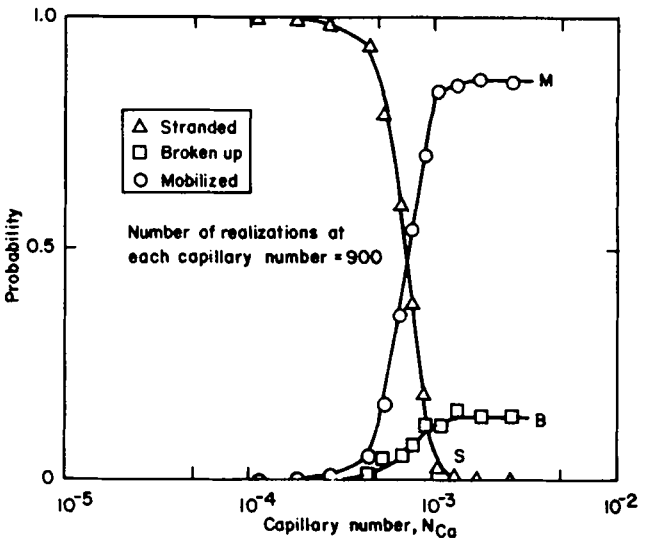

Figure 9. Plot of the probabilities of mobilization M, breakup per rheon B and stranding per rheon S for fifteen CEVS ganglia in a 100 × 200 sandpack vs. capillary number.

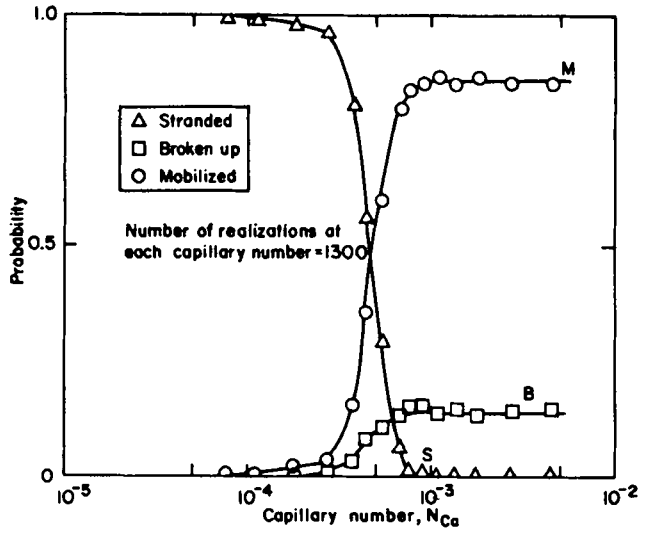

Figure 10. Plot of the probabilities of mobilization M, breakup per rheon B and stranding per rheon S for twenty-eight CEVS ganglia in a 100 × 200 sandpack vs. capillary number.

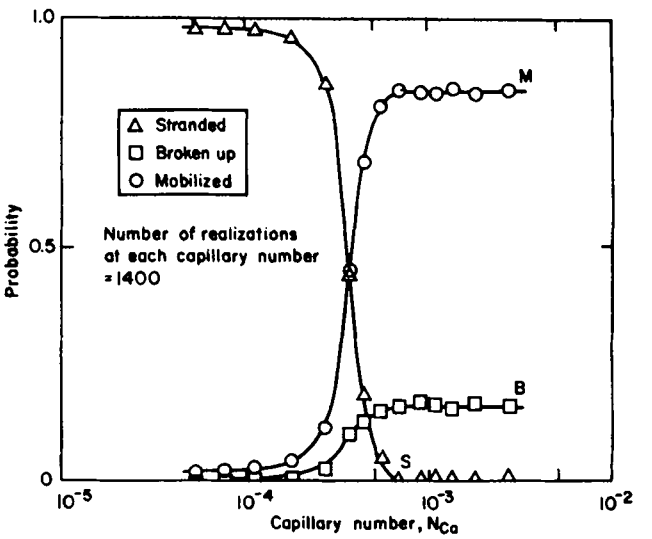

Figure 11. Plot of the probabilities of mobilization M, breakup per rheon B and stranding per rheon S for forty-two CEVS ganglia in a 100 × 200 sandpack vs. capillary number.

From the preceding analysis it becomes clear that for a given porous medium the probabilities M, B and S are functions of ganglion size and capillary number N_{Ca}. They can be calculated readily by making a large number (say a few hundred) realizations with the algorithm given earlier in this paper, but stopping each realization after the first rheon. By simple enumeration of the various outcomes and formation of the occurrence fraction for each outcome, one obtains the values of M, B and S for the particular ganglion size and capillary number (for the porous medium under consideration).

A related variable of fundamental importance (see Payatakes, Ng and Flumerfelt, 1980) is the breakup mode probability, which is defined as

$$W(u,v)\Delta v = Pr\{\text{A moving u ganglion divides into two daughter ganglia, one of which is a v ganglion, given that the u ganglion is undergoing fission}\} \quad (29)$$

This probability can also be calculated from the same set of realizations used to calculate M, B and S.

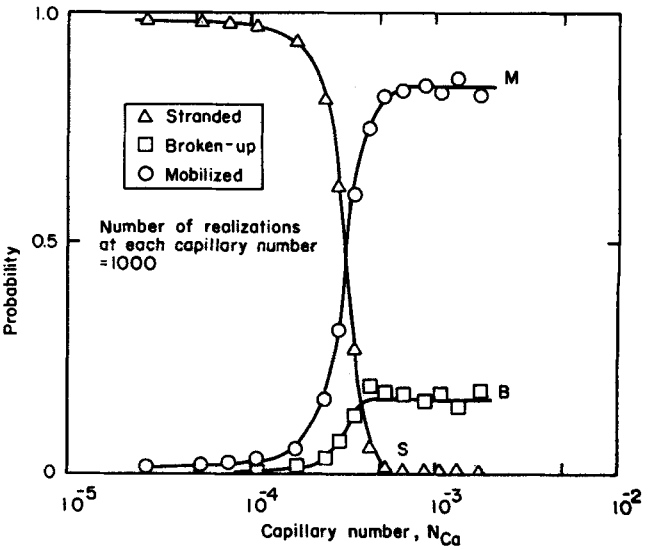

Figure 12. Plot of the probabilities of mobilization M, breakup per rheon B and stranding per rheon S for fifty-one CEVS ganglia in a 100 × 200 sandpack vs. capillary number.

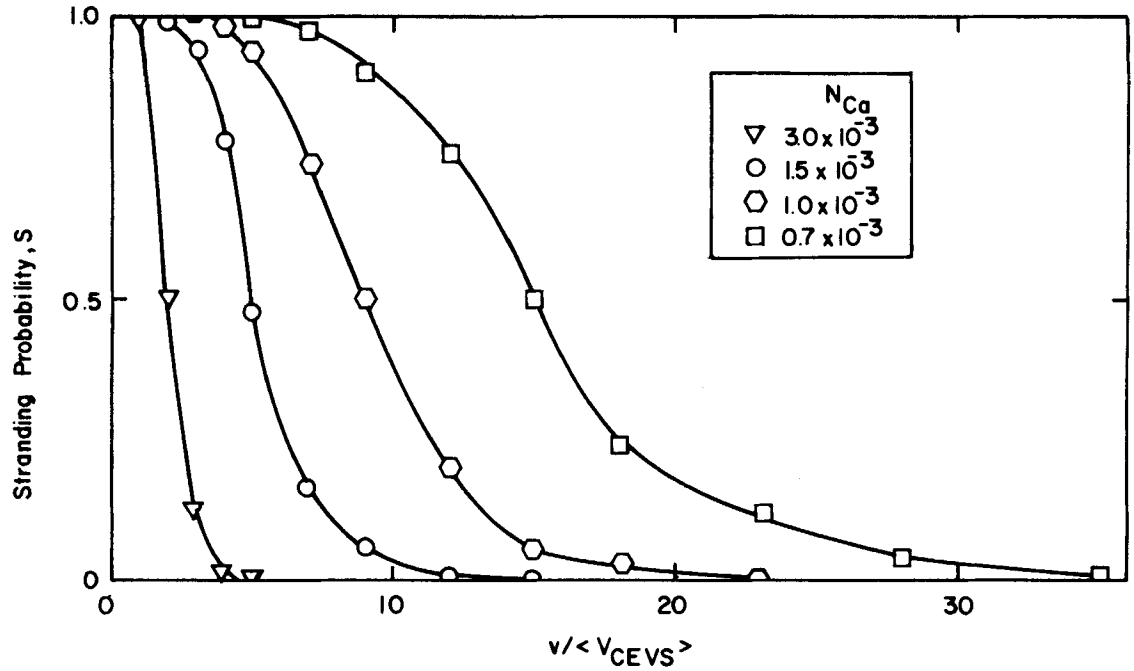

Figure 13. Plot of the probability of stranding per rheon S vs. dimensionless ganglion size for various capillary numbers.

Sample Calculations of the Probabilities M, B, S and W

To demonstrate the feasibility and utility of the method, we calculated M, B, S and W for a 100 × 200 sandpack, $\theta = 0$ and ganglia sizes from one to fifty-one CEVS over the entire range of capillary numbers of interest. Typical M, B and S vs. N_{Ca} results are plotted in Figures 4 to 12. The dependence of S on ganglion size is given in Figure 13 for several capillary number values. $W\Delta v$ vs. v results are plotted in Figure 14. Plots 4 to 14 were obtained for solitary ganglia but apply equally well to members of large ganglia populations. The only adjustment necessary is in calculating the capillary number value to be used in reading the plots. The value of N_{Ca}/k_{rw} should be used, rather than that of N_{Ca}, in order to compensate for the increase in the pressure gradient required to maintain the same value of the superficial velocity of the aqueous phase V_f. An analytical expression giving the relative permeability k_{rw} as function of water saturation S_w was developed in Payatakes, Ng and Flumerfelt (1980).

Some interesting conclusions can be drawn from these calculations:

1. For each ganglion size, there is a critical capillary number below which the stranding probability per rheon, S, is non-negligible.

2. The probability of stranding per rheon is virtually unity at small capillary numbers (as expected) and decreases rapidly with N_{Ca} and ganglion size; it is negligible for large ganglia (say > ten CEVS and $N_{Ca} > 3 \times 10^{-3}$ (in complete agreement with previous work).

3. Once the probability of mobilization M becomes finite, the probability of breakup per rheon B becomes finite too (except for one CEVS ganglia).

4. The probability of breakup per rheon B rises in a relatively small range of capillary number values from nil to a constant value. The plateau begins at the point where the stranding probability S virtually vanishes. The plateau value of B is ~0.02 for two CEVS ganglia, goes through a maximum of 0.17 for three CEVS and four CEVS ganglia and remains in the range 0.10 to 0.17 for larger ganglia.

5. The implication from observations (3) and (4) is that mobilized solitary ganglia (≥ two CEVS) are destined to either get restranded whole or to break up in daughter ganglia, which subsequently get stranded. One of these terminal events is expected to happen after relatively few rheons (no more than thirty to fifty).

6. In a population of noninteracting ganglia, significant oil recovery can only be expected for capillary numbers larger than the value effecting complete mobilization ($M = 1$) of one CEVS ganglia, that is, $N_{Ca} > \sim 10^{-2}$.

7. The breakup of large oil ganglia is much more likely to produce daughter ganglia of widely different sizes (one large, one small) than daughter ganglia of comparable sizes, Figure 14. This, of course, was expected, in view of the fact that breakup occurs at thin ganglion sections, which are rare in the middle of large ganglia. They usually occur at peripheral appendages.

These conclusions suggest rather clearly the reasons for which the ganglion population balance approach developed in Payatakes, Ng and Flumerfelt (1980) is necessary to analyze the phenomena associated with oil-bank formation and/or attrition.

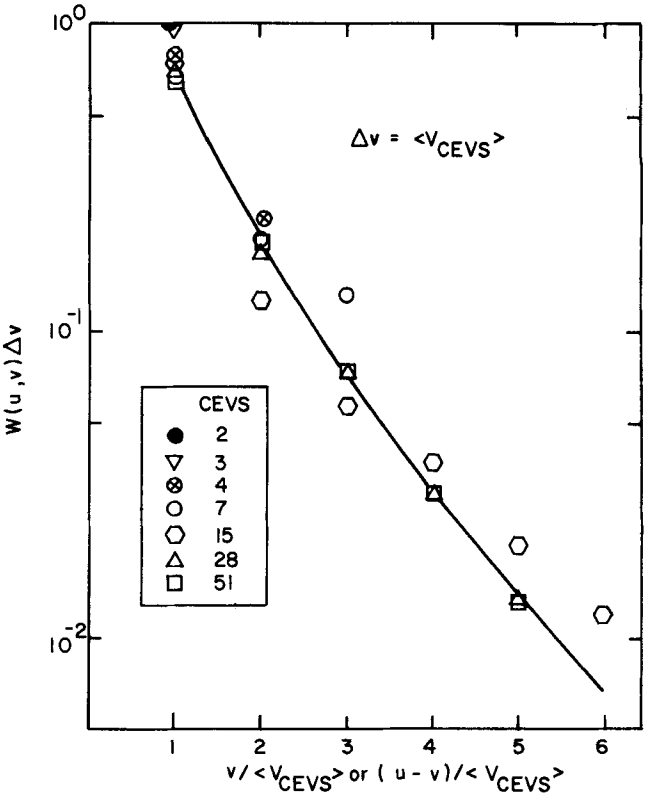

Figure 14. Plot of the breakup mode probability vs. daughter ganglion size v with the mother ganglion size u as parameter. The symmetrical right half of the plot is not shown.

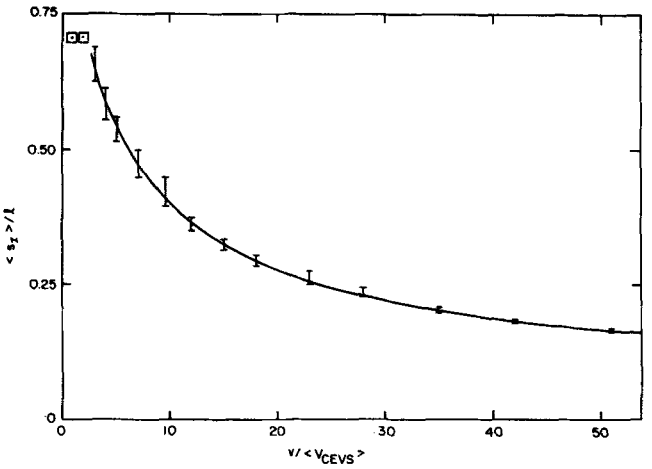

Figure 15. Plot of the normalized expected axial distance traveled per rheon vs. dimensionless ganglion size. The bars indicate systematic decrease of s_z/ℓ with increasing capillary number in the range of capillary numbers investigated ($10^{-4}<N_{Ca}<10^{-2}$).

THE STRANDING COEFFICIENT λ AND THE BREAKUP COEFFICIENT ϕ

Payatakes, Ng and Flumerfelt (1980) expressed the effects of stranding and breakup on oil ganglion dynamics in terms of the stranding coefficient λ and the breakup coefficient ϕ. These are defined by

$$\left.\frac{\partial n}{\partial z}\right)_{\text{due to stranding}} = -\lambda n \tag{30}$$

$$\left.\frac{\partial n}{\partial z}\right)_{\text{due to breakup}} = -\phi n \tag{31}$$

It can be shown (see appendix) that λ and ϕ are given by

$$\lambda = -\frac{S}{(1-M)}\frac{\ln M}{s_z} \tag{32}$$

$$\phi = -\frac{B}{(1-M)}\frac{\ln M}{s_z} \tag{33}$$

where s_z can be easily determined from stochastic simulations.

Sample Calculations of s_z, λ and ϕ

Profiles of s_z, λ and ϕ for a 100 × 200 sandpack and $\theta = 0$, calculated from computer simulations and Equations (32) and (33), are plotted in Figures 15, 16, and 17, respectively. As can be seen, s_z is a monotonically decreasing function of ganglion size, since a single rheon has a diminishing effect on the coordinates of the centroid of the ganglion, as the size of the latter increases. The stranding coefficient λ, which has dimensions of inverse length, is, as expected, a monotonically decreasing function of N_{Ca} and ganglion size. The breakup coefficient ϕ has also dimensions of inverse length and increases with ganglion size, at least in the range investigated. This would be a much more serious danger were it not for the fact that, as Figure 14 shows, large ganglia usually lose only small parts of their body during each fission and therefore retain their volumes relatively intact. On the other hand, collison and coalescence between two large ganglia is a significant (for them) event, substantially assisting the two merging ganglia to contribute to oil bank formation.

Figure 14, together with Figures 4 to 13, explains the origin of the one to ten CEVS ganglia that comprise the main volume of residual oil at the end of secondary flooding. These small ganglia are generated by breakup from larger oil blobs (attrition) and almost immediately fall behind and get stranded owing to the small capillary number which characterizes secondary floods (say $N_{Ca} \cong 10^{-5}$).

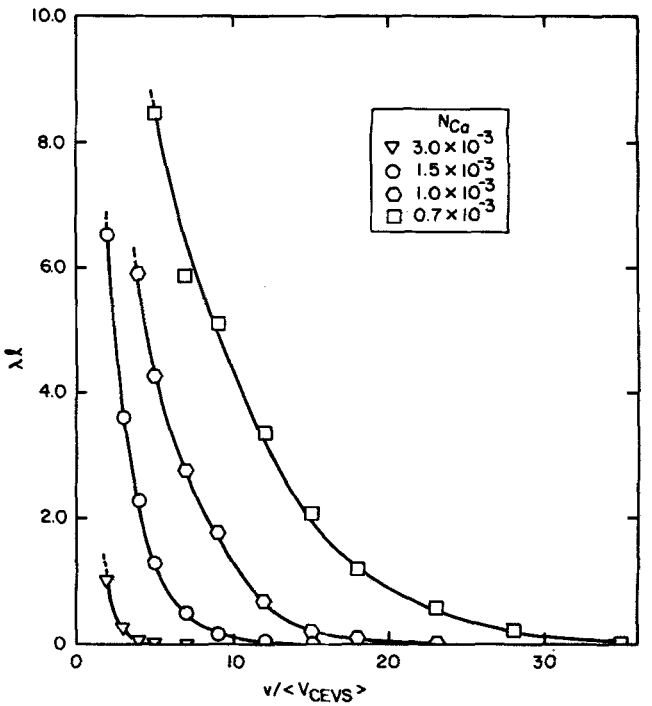

Figure 16. Plot of the dimensionless stranding coefficient vs. dimensionless ganglion size for various capillary numbers.

AXIAL AND LATERAL GANGLION DISPERSION COEFFICIENTS

An order of magnitude estimate of D_x and D_z for v ganglia can be obtained as follows. Consider a v ganglion during the period between time $t=0$, when it gets mobilized, and the time when it gets stranded, or it fissions. Assume that the ganglion undergoes rheons at constant time intervals $<t_r>$ and that during each rheon the center of gravity of the oil ganglion is displaced by a distance Δz in the axial direction z and by a distance Δx in the lateral direction x (we consider here the simplified two-dimensional network case). Both Δz and Δx are random variables, but whereas Δz is always positive and has expected value $<\Delta z> = s_z>0$, Δx can be either positive or negative and $<\Delta x>=0$. Consider now an observer that starts moving with the ganglion at $t = 0$ but travels with constant velocity $\bar{u}_z(v;a_1)$. Relative to this observer, the v ganglion executes a random walk, which can be considered as being composed of two random walks, one along z and one along x. We set then

$$D_x \cong \frac{\overline{(\Delta x - <\Delta x>)^2}}{2<t_r>} = \frac{\overline{(\Delta x)^2}}{2<t_r>} \tag{34}$$

and

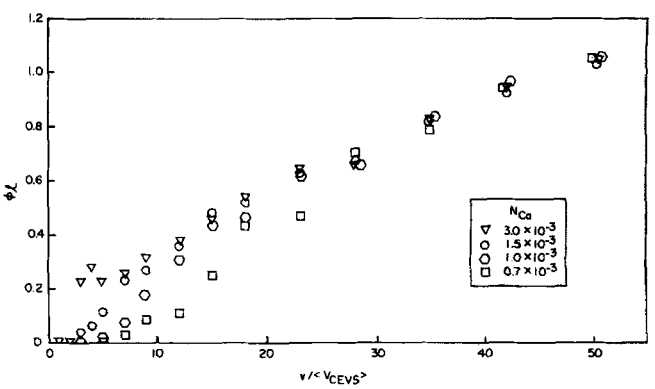

Figure 17. Plot of the dimensionless breakup coefficient vs. dimensionless ganglion size for various capillary numbers.

$$D_z \cong \frac{\overline{(\Delta z - <\Delta z>)^2}}{2<t_r>} = \frac{[\overline{(\Delta z)^2} - <\Delta z>^2]}{2<t_r>}$$

$$= \frac{[\overline{(\Delta z)^2} - s_z^2]}{2<t_r>} \quad (35)$$

where we have set $\overline{\Delta z} = <\Delta z>$. Observing now that $\bar{u}_z = s_z/<t_r>$, we get

$$D_x \cong \bar{u}_z \frac{\overline{(\Delta x)^2}}{2s_z} \quad (36)$$

$$D_z \cong \bar{u}_z \frac{[\overline{(\Delta z)^2} - s_z^2]}{2s_z} \quad (37)$$

Since $\overline{(\Delta x)^2}$ and $\overline{(\Delta z)^2}$ can be obtained readily from the same realizations used to determine M, B, S and s_z, the problem of calculating D_x and D_z is reduced to that of determining $\bar{u}_z$. Once again, the average ganglion velocity $\bar{u}_z$ emerges as a key parameter in this model (see also Payatakes, Ng and Flumerfelt, 1980). It is very unfortunate that there is only scarce experimental information and no theoretical analysis concerning $\bar{u}_z$. This may be due, in part, to the fact that without benefit of a model such as the present one, the need for correlations or theoretical expressions for $\bar{u}_z$ had not been felt. An attempt to study this problem theoretically is confronted immediately by great difficulties, and a successful solution will certainly require a major effort. Work is currently underway at our laboratory to obtain at least an experimental correlation, giving $\bar{u}_z$ as a function of ganglion size, porous medium geometry and operational and physicochemical variables.

It should be pointed out here that Equations (36) and (37) are only rough approximations which are based on a number of assumptions, not least of which is the premise that the waiting time for each rheon is always the same. Actually, the waiting time for a rheon t_r is a random variable, and this factor contributes to further increase the effective dispersion coefficient values.

ACKNOWLEDGMENT

This work was performed under U. S. Department of Energy Grant No. E(40-1)-5075, with support from Shell Oil Company and Marathon Oil Company. We thank Dr. James C. Melrose and Dr. Carl F. Brandner of Mobil Research and Development and Dr. Elmond Claridge of Shell Development for valuable discussions.

NOTATION

a_i = maximum diameter of the extended i^{th} gate unit cell
$\underline{a}_1, \underline{a}_2$ = parameter vectors
$B(v;\underline{a}_2)$ = probability of breakup of a v ganglion per rheon
$D_z(v;\underline{a}_1)$, $D_x(v;\underline{a}_1)$ = axial and lateral dispersion coefficients for moving v ganglia
d_i = minimum diameter of the i^{th} unit cell
G = $|\nabla P|$
G_{cr} = critical value of $|\nabla P|$ at which a given ganglion gets mobilized
I = index of the gate unit cell through which the xeron takes place
i,j = dummy indices used to identify gate unit cells (or throats)
$J_{dr,i}$ = drainage curvature in the i^{th} gate unit cell
$J^0_{dr,i}$ = value of $J_{dr,i}$ for zero contact angle
J_i = interface curvature in the i^{th} gate unit cell
$J_{lb,j}$ = lower bound of interfacial curvature in the (extended) j^{th} gate unit cell, Equation (5)
$J_1^{(j)}$ = curvature defined by Equation (6)
$J_{1,min}$ = curvature defined by Equation (7)
K = index of the gate unit cell through which the hygron takes place
k_{rw} = relative permeability to water
L_p = maximum ganglion length projected on the main flow direction
ℓ = length of periodicity of the porous medium
$M(v;\underline{a}_2)$ = probability that a v ganglion will undergo at least one rheon from its present position
N_{am} = appendix mobilization number, Equation (23)
$N_{Ca} = \mu_w V_f/\gamma_{ow}$ = capillary number
N_{guc} = number of gate unit cells of a given ganglion
$n(z,t;v)\Delta v$ = number of moving v ganglia per unit reservoir volume
n_0 = initial value of n in the derivation of λ and ϕ (see Appendix)
P = pressure
P_{oi}, P_{wi} = pressure in the oil and water phases, respectively, next to the interface in the i^{th} gate unit cell
$S(v;\underline{a}_2)$ = probability that a v ganglion introduced randomly in the porous medium will find itself stranded before a single rheon takes place
S_w = water saturation
s_z = expected length of travel of the center of gravity of a v ganglion in the axial direction, per rheon
t = time measured from the initiation of the flood
t_r = waiting time for a rheon (time between successive rheons)
$\bar{u}_z(v;\underline{a}_1)$ = mean velocity of the centers of gravity of v-ganglia in the axial direction
V_f = superficial velocity of the flood
$W(u, v)\Delta v$ = probability that a moving u ganglion undergoing fissioning will break into two daughter ganglia, one of which is a v ganglion
x = lateral Cartesian coordinate
z = Cartesian coordinate in the direction of the flood

Greek Letters

$\beta(z,t;v)\Delta v$ = number of fission events that have happened to a traveling slug of v ganglia, per unit volume (see Appendix)
β_{Ki} = appendix mobility factors, Equation (16)
β_{KI} = maximum value among β_{Ki} for a given ganglion
γ_{ow} = interfacial tension at the oil-water interface
ΔL_{ij} = distance between two constrictions, denoted by i and j, for a given ganglion
δ = thickness of the traveling slug of v ganglia (see Appendix)
ϵ = porosity
θ = apparent contact angle, as measured from the wetting phase
θ_{ij} = angle between the line connecting gate constriction i to gate constriction j and the macroscopic flow direction
$\lambda(v;\underline{a}_2)$ = stranding coefficient
μ_w = dynamic viscosity of water
$\sigma(z,t;v)\Delta v$ = number of stranded v ganglia per unit volume
τ = transformed time, Equation (A2)
$\phi(v;\underline{a}_2)$ = breakup coefficient

LITERATURE CITED

Healy, R. N., and R. L. Reed, "Physiocochemical Aspects of Microemulsion Flooding," *Soc. Petrol. Eng. J.*, **14**, 491 (1974).

Healy, R. N., R. L. Reed, and D. G. Stenmark, "Multiphase Microemulsion Systems," *ibid.*, **16**, 147 (1976).

Melrose, J. C., "Wettability as Related to Capillary Action in Porous Media," *ibid.*, **5**, 259 (1965).

Melrose, J. C. and C. F. Brandner, "Role of Capillary Forces in Determining Microscopic Displacement Efficiency for Oil Recovery by Waterflooding," *Can. J. Petrol. Technol.*, **13**, No. 4, 54 (1974).

Nelson, R. C., and G. A. Pope, "Phase Relationships in Chemical Flooding," SPE 6773, 52nd Annual Fall Technol. Conf. and Exhib. SPE, Denver, Colo. (Oct. 9-12, 1977).

Payatakes, A. C., R. W. Flumerfelt and K. M. Ng, "Model of Isotropic Granular Porous Media for the Simulation of Oil Ganglia Motion, Partition and Coalescence During Immiscible Displacement," paper presented at AIChE 70th Annual Meeting, New York (Nov. 13-17, 1977).

Payatakes, A. C., R. W. Flumerfelt, and K. M. Ng, "On the Dynamics of Oil Ganglia Populations During Immiscible Displacement," paper presented at AIChE 84th National Meeting, Atlanta, Ga. (Feb. 26—Mar. 1, 1978a).

Payatakes, A. C., R. W. Flumerfelt and K. M. Ng, "Oil Ganglia Dynamics During Immiscible Displacement. Effects of Interfacial Properties," *Proc. 4th DOE Symposium on Enhanced Oil and Gas Recovery*, Tulsa, Okla. (Aug. 29-31, 1978*b*).

Payatakes, A. C., K. M. Ng and R. W. Flumerfelt, "Oil Ganglia Dynamics During Immiscible Displacement. Model Formulation," *AIChE J.*, **26**, 430 (1980).

Wasan, D. T., K. Sampath, J. J. McNamara, et al., "The Mechanism of Oil Bank Formation, Coalescence in Porous Media and Emulsion Stability," *Proc. 4th DOE Symposium on Enhanced Oil and Gas Recovery*, Tulsa, Okla. (Aug. 29-31, 1978).

Wasan, D. T., J. J. McNamara, S. M. Shah, et al., "The Role of Coalescence Phenomena and Interfacial Rheological Properties in Enhanced Oil Recovery: An Overview," *J. of Rheology*, **23**, No. 2, 181 (1979).

APPENDIX

Derivation of Equations (32) and (33)

Consider an initial population of v ganglia distributed between two planes, which are normal to the main flow direction z and are separated by a small distance δ. The distance δ is assumed to be comparable to s_z. Assume that at time $t = 0$ an immiscible flood with superficial velocity V_f starts flowing past the oil ganglia. If we neglect axial dispersion (which is permissible for a small distance), we conclude that the v ganglion population will begin migrating downstream as a slug with velocity $\bar{u}_z(v;\underline{a}_1)$, being however decimated in the process by stranding and breakup.

Subject to the assumptions of the present analysis, the population balance equation for moving v ganglia developed in Payatakes, Ng and Flumerfelt (1980) is reduced to

$$\frac{\partial n(z,t;v)}{\partial t} + \bar{u}_z(v;\underline{a}_1)\frac{\partial n(z,t;v)}{\partial z} = -\bar{u}_z(v;\underline{a}_1)\,[\lambda(v;\underline{a}_2) + \phi(v;\underline{a}_2)]n(z,t;v) \tag{A1}$$

Let a transformed time variable τ be defined as

$$\tau = t - \frac{z}{\bar{u}_z(v;\underline{a}_1)} \tag{A2}$$

Clearly, τ is constant for an observer moving with the slug of v ganglia. It can be shown easily that Equation (A1) is transformed into

$$\left[\frac{\partial n(z,\tau;v)}{\partial z}\right]_\tau = -[\lambda(v;\underline{a}_2) + \phi(v;\underline{a}_2)]n(z,\tau;v) \tag{A3}$$

Integrating, we get

$$n(z,\tau;v) = n_0\exp[-(\lambda+\phi)z]\,;\ \text{(moving v ganglia)} \tag{A4}$$

where n_0 is the initial value of n.

We proceed now to make an overall v ganglion balance as follows. Consider the v ganglion slug first at position z and then at a downstream position $z + \Delta z$, where Δz is assumed to be relatively small (say, $\Delta z < 10\ell$. For a cross-sectional area A_c, we have

$$\left\{\begin{matrix}\text{total number of moving}\\ \text{v ganglia casualties}\\ \text{along the length } \Delta z\end{matrix}\right\} = -A_c\delta[n(z+\Delta z,\tau;v) - n(z,\tau;v)]\Delta v \tag{A5}$$

$$\left\{\begin{matrix}\text{number of v ganglia}\\ \text{stranded along the}\\ \text{length } \Delta z\end{matrix}\right\} = A_c\Delta z\sigma(z+\eta_1\Delta z,\tau;v)\Delta v \tag{A6}$$

$$\left\{\begin{matrix}\text{number of v ganglia}\\ \text{that fissioned along}\\ \text{the length } \Delta z\end{matrix}\right\} = A_c\Delta z\beta(z+\eta_2\Delta z,\tau;v)\Delta v \tag{A7}$$

where $n(z,\tau;v)\Delta v$ is the number of moving v ganglia per unit volume, $\sigma(z,\tau;v)\Delta v$ is the number of stranded v ganglia per unit volume, $\beta(z,\tau;v)\Delta v$ is the number of v ganglion fissions per unit volume and η_1, η_2 are some position constants from the interval (0,1).

An overall v ganglion balance gives

$$-\delta\frac{n(z+\Delta z,\tau;v) - n(z,\tau;v)}{\Delta z} = \sigma(z+\eta_1\Delta z,\tau;v) + \beta(z+\eta_2\Delta z,\tau;v)$$

Letting $\Delta z \to 0$, we get

$$-\delta\left(\frac{\partial n}{\partial z}\right)_\tau = \sigma + \beta\,;\ \text{(overall v ganglion balance)} \tag{A8}$$

Equations (A3) and (A8) together give

$$\sigma + \beta = \delta(\lambda+\phi)n \tag{A9}$$

Since σ and β are proportional to λ and ϕ, respectively, all other factors being the same, we have

$$\frac{\sigma}{\beta} = \frac{\lambda}{\phi} \tag{A10}$$

Solving Equations (A9) and (A10) for σ and β, we get

$$\sigma = \delta\lambda n = \delta\lambda n_0\exp[-(\lambda+\phi)z] \tag{A11}$$

$$\beta = \delta\phi n = \delta\phi n_0\exp[-(\lambda+\phi)z] \tag{A12}$$

In order to connect λ and ϕ to the basic probabilities M, B and S, we consider the progression of the v ganglia slug as a random walk process.

Clearly, the expected concentration of moving v ganglia after n rheons is n_0M^n. This expression is set equal to the value predicted by Equation (A4) to get

$$n_0M^n = n_0\exp[-(\lambda+\phi)ns_z]$$

Solving for $(\lambda + \phi)$, we obtain

$$\lambda + \phi = -\frac{1}{s_z}\ln M \tag{A13}$$

We proceed by making a stranded ganglion balance considering only one rheon. We get

$$\delta(n\Delta v)A_cS = \int_z^{z+s_z}(\sigma\Delta v)A_c\,dz$$

Invoking Equation (A11), we get

$$\delta nS = \int_z^{z+s_z}\sigma dz = \delta n_0\lambda\int_z^{z+s_z}\exp[-(\lambda+\phi)z]dz$$

$$= \delta n_0\frac{\lambda}{(\lambda+\phi)}\exp[-(\lambda+\phi)z]\{1-\exp[-(\lambda+\phi)s_z]\}$$

If we recall Equation (A4), the last equation reduces to

$$S = \frac{\lambda}{(\lambda+\phi)}\{1-\exp[-(\lambda+\phi)s_z]\} \tag{A14}$$

Equations (A13) and (A14) give

$$S = \frac{\lambda}{(\lambda+\phi)}(1-M) \tag{A15}$$

Similarly, we get

$$B = \frac{\phi}{(\lambda+\phi)}(1-M) \tag{A16}$$

Dividing Equations (A15) and (A16), we also get

$$\frac{S}{B} = \frac{\lambda}{\phi} \tag{A17}$$

Equations (A13) and (A17) can be solved for λ and ϕ to get Equations (32) and (33).

Manuscript received January 17, 1979, and accepted October 11, 1979.